

cial shear stress provides the necessary boundary condition for viscoelastic deformation rather than the thermodynamic work of adhesion.

According to this simple picture of energy dissipation at the crack tip, the shear stress at the FC surface turns out to be about four to six times that of the HC surface (see Fig. 1). Interestingly, similar ratios of shear stresses were observed in the direct measurement (9) of the interfacial friction of several materials against FC and HC monolayers.

The ratio  $\eta/G$  in Eq. 4 is the slow response time (21) of the adhesive, which is  $\sim 2$  to 3 s. The value of  $\alpha$  is  $\sim 10$  to 15 (22). If we use the shear stresses (1 to 100 kPa) of rubber sliders (9, 10, 23) against rigid walls as the approximate values of  $\sigma_s$ ,  $G_0$  is estimated to be in the range of 4 to 400 N/m for  $u = 100 \mu\text{m/s}$ . The experimentally observed peel forces fall well within this range. This kind of quantitative comparison, however, should not be taken too far, because the equations for the viscous energy dissipation (Eqs. 3 and 4) are strictly valid for low contact angles (or high  $\sigma_s$ ), that is, Fig. 3C. Furthermore, our model does not include extensional deformation of the adhesive. Nevertheless, this simple calculation shows that the local viscous energy dissipation at the crack tip can be quite substantial, and its magnitude decreases as the interfacial slipage increases.

## REFERENCES AND NOTES

- A. N. Gent and J. Schultz, *J. Adhes.* **3**, 281 (1972).
- E. H. Andrews and A. J. Kinloch, *Proc. R. Soc. London Ser. A* **332**, 385 (1973); R. J. Good and R. K. Gupta, *J. Adhes.* **26**, 13 (1988).
- Both the hydrocarbon and fluorocarbon monolayers were prepared by reacting the silicon wafer to the vapor of alkyltrichlorosilanes  $[\text{CH}_3(\text{CH}_2)_n\text{SiCl}_3]$ ,  $9 \leq n \leq 15$  and fluoroalkyltrichlorosilane  $[\text{CF}_3(\text{CF}_2)_{7-9}(\text{CH}_2)_2\text{SiCl}_3]$  according to the methods described by M. K. Chaudhury and G. M. Whitesides [*Langmuir* **7**, 1013 (1991)]. PDMS  $[\text{CH}_3\text{CH}_2\text{CH}_2\text{CH}_2\text{OSi}(\text{CH}_3)_2(\text{CH}_3)_2\text{SiH}]$  was chemically grafted to the silicon wafer by reacting its Si-H groups to the surface silanols by using a platinum catalyst. Two PDMS polymers with weight-average molecular weights of 8612 and 33187 were used to yield films of thickness 50 and 100 Å, respectively.
- The surfaces were examined with two liquids, water and hexadecane. The advancing ( $\theta_a$ ) and receding ( $\theta_r$ ) contact angles were PDMS (water:  $\theta_a = 108^\circ$ ,  $\theta_r = 106^\circ$ ; hexadecane:  $\theta_a = 42^\circ$ ,  $\theta_r = 32^\circ$ ), HC (water:  $\theta_a = 114^\circ$  to  $117^\circ$ ,  $\theta_r = 108^\circ$  to  $112^\circ$ ; hexadecane:  $\theta_a = 44^\circ$  to  $46^\circ$ ,  $\theta_r = 43^\circ$  to  $45^\circ$ ), and FC (water:  $\theta_a = 118^\circ$ ,  $\theta_r = 106^\circ$ ; hexadecane:  $\theta_a = 81^\circ$ ,  $\theta_r = 75^\circ$ ). The surface free energy was estimated from the average of the advancing and receding contact angles of hexadecane and by using the equation of Good, Girifalco, and Fowkes [L. A. Girifalco and R. J. Good, *J. Phys. Chem.* **61**, 904 (1957); F. M. Fowkes, *Ind. Eng. Chem.* **56**, 40 (1964)].
- K. L. Johnson, K. Kendall, A. D. Roberts, *Proc. R. Soc. London Ser. A* **324**, 301 (1971).
- A standard 3M scotch tape (catalog number of 34-7032-3525-8) was used as the adhesive material.
- K. B. Migler, H. Hervet, L. Leger, *Phys. Rev. Lett.* **70**, 287 (1993); K. B. Migler, G. Massey, H. Hervet, L. Leger, *J. Phys. Condens. Matter* **6**, A301 (1994), and references therein.
- G. Reiter, A. L. Demirel, J. Peanasky, L. L. Cai, S. Granick, *J. Chem. Phys.* **101**, 2606 (1994); G. Reiter, A. L. Demirel, S. Granick, *Science* **263**, 1741 (1994).
- B. J. Briscoe and D. C. B. Evans, *Proc. R. Soc. London Ser. A* **380**, 389 (1982); V. DePalma and N. Tillman, *Langmuir* **5**, 868 (1989); R. M. Overney *et al.*, *Nature* **359**, 133 (1992).
- M. K. Chaudhury and M. J. Owen, *Langmuir* **9**, 29 (1993).
- H. R. Brown, *Science* **263**, 1411 (1994).
- The phase states of the monolayer were varied by controlling the concentration of the silane in the vapor phase. Details can be found in M. K. Chaudhury and M. J. Owen, *J. Phys. Chem.* **97**, 5722 (1993).
- M. D. Thouless and H. M. Jensen, *J. Adhes.* **38**, 185 (1992).
- J. W. Hutchinson and Z. Suo, *Adv. Appl. Mech.* **29**, 63 (1992).
- R. J. Fields and M. F. Ashby, *Philos. Mag.* **33**, 33 (1976).
- Y. Urahama, *J. Adhes.* **31**, 47 (1989).
- A. Zosel, *ibid.* **34**, 201 (1991).
- E. P. Chang, *ibid.*, p. 189.
- V. E. Dussan and S. Davis, *J. Fluid Mech.* **65**, 71 (1974).
- P. G. de Gennes, *Rev. Mod. Phys.* **57**, 828 (1985).
- The response time of the adhesive was estimated by studying the free relaxation of the Schallamach ridges [A. Schallamach, *Proc. R. Soc. London Ser. B* **66**, 386 (1953)], which were formed by sliding a rubber slider over the adhesive.
- T. Ondarcuhu and M. Veysie, *J. Phys. Paris* **111**, 75 (1991).
- M. Barquins, *Mater. Sci. Eng.* **73**, 45 (1985).
- M.K.C. thanks A. N. Gent for valuable discussions. We thank Dow Corning Corporation and IBM for supporting this work.

26 April 1995; accepted 27 June 1995

## Direct Evaluation of Electronic Coupling Mediated by Hydrogen Bonds: Implications for Biological Electron Transfer

Peter J. F. de Rege, Scott A. Williams,\* Michael J. Therien†

Three supramolecular bischromophoric systems featuring zinc(II) and iron(III) porphyrins have been synthesized to evaluate the relative magnitudes of electronic coupling provided by hydrogen,  $\sigma$ , and  $\pi$  bonds. Laser flash excitation generates the highly reducing singlet excited state of the (porphinato)zinc chromophore that can subsequently be electron transfer quenched by the (porphinato)iron(III) chloride moiety. Measurement of the photoinduced electron transfer rate constants enables a direct comparison of how well these three types of chemical interactions facilitate electron tunneling. In contrast to generally accepted theory, electronic coupling modulated by a hydrogen-bond interface is greater than that provided by an analogous interface composed entirely of carbon-carbon  $\sigma$  bonds. These results bear considerably on the analysis of through-protein electron transfer rate data as well as on the power of theory to predict the path traversed by the tunneling electron in a biological matrix; moreover, they underscore the cardinal role played by hydrogen bonds in biological electron transfer processes.

Ascertaining how the structural complexities of proteins and membranes impact long-range donor-acceptor (D-A) interactions has long been a primary focus for both theory and experiment in the field of biological electron transfer (ET) (1). Beratan and Onuchic recognized that the anisotropic nature of the protein medium likely gave rise to significant variations in how well distinct regimes of polypeptide secondary and tertiary structure effected the propagation of a tunneling electron wave function (2). These theoretical studies led to the development of algorithms to estimate the magnitude of electronic coupling between redox sites in a biological matrix as well as predict the pathway traversed by the tunneling electron (3). This "pathway model" for biological electron transport relies on

the premise that covalent bonds, hydrogen (H) bonds, and van der Waals contacts between atoms all modulate electronic coupling differently; hence, the extent of the decay of the tunneling electron wave function (that is, the electronic coupling between D and A) depends critically on the number of each of these chemical interactions that defines a physical ET pathway connecting D to A.

Since the first through-protein ET experiments demonstrating that the pathway model correctly predicted a specific H-bonding interaction to be critical in establishing long-range D-A electronic coupling (4), this method of theoretical analysis has provided (i) insight into the nature of the groups of atoms that comprise the important ET pathways in biological systems and (ii) a basis for rationalizing the magnitude of experimental ET rate constants for redox reactions involving the cytochromes (5), azurin (6), catalase (7), protein-protein complexes (8), the photosynthetic reaction center (9), as well as peptide

Department of Chemistry, University of Pennsylvania, Philadelphia, PA 19104-6323, USA.

\*Present address: Department of Imaging and Photographic Technology, Rochester Institute of Technology, Rochester, NY 14623, USA.

†To whom correspondence should be addressed.

and nucleic acid oligomers (10).

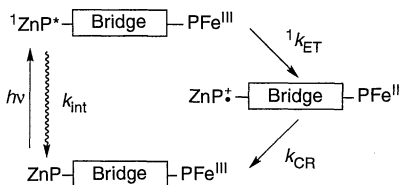
Although indirect evidence shows that H bonds play crucial roles in facilitating through-protein electronic coupling (5–10) and recent work in well-defined chemical systems indicates that H-bonded interfaces are certainly competent to be an integral component of the medium in long-range biological ET reactions (11, 12), the effect H-bonded interactions have on the tunneling barrier has not yet been evaluated. Enhancing the predictive power of ET theory with respect to biological charge transfer processes requires more sophisticated electronic models of the biological media; to this end, we have synthesized three ET model systems in which the tunneling barrier between D and A is varied systematically.

The C–C single bond and the C=C double bond were chosen as electronic coupling benchmarks for the H bond; the ET model systems we constructed to effect these comparisons are shown in Fig. 1. The supramolecular complexes  $1(\text{Zn}^{\text{II}}, \text{Fe}^{\text{III}})$ ,  $2(\text{Zn}^{\text{II}}, \text{Fe}^{\text{III}})$ , and  $3(\text{Zn}^{\text{II}}, \text{Fe}^{\text{III}})$  feature (porphinato)zinc donors and (porphinato)iron(III) chloride acceptors separated by a virtually constant distance, thus establishing uniform driving force and reorganization energy for the ET reaction (13). These systems fix the number of bonds in the medium, keeping the steps in the ET reaction identical. The locations of the electronic perturbations to the tunneling medium are well separated from both D and A, ensuring that such modifications impact only the tunneling barrier and not the reactant-product electronic states or the nature of the initial D–A coupling onto the bridge (medium). The bridges that connect D to A are rigid, guaranteeing a constant D–A distance. Steric interactions between the aryl ring ortho and porphyrin  $\beta$  hydrogen atoms are substantial, fixing the D–A (porphyrin) orientation with respect to the bridge (14). The [3.3.0] bicyclic structure is specifically cis and conformationally inflexible. Table 1 describes how each of the bridging moieties in these ET models affects D–A orientation and distance.

The D–A assembly  $1(\text{Zn}^{\text{II}}, \text{Fe}^{\text{III}})$  forms in aprotic solvent through the complementary association of the two benzoic acid–derivatized porphyrins,  $4(\text{Zn}^{\text{II}})$  and  $4(\text{Fe}^{\text{III}})$  (15–17). Photoexcitation of  $4(\text{Zn}^{\text{II}})$  at 560 nm produces the highly reducing singlet excited state of the molecule ( $^1\text{ZnP}^*$ ); in the absence of any added  $4(\text{Fe}^{\text{III}})$ , this species has an intrinsic fluorescent lifetime of 1.42 ns. In the presence of  $4(\text{Fe}^{\text{III}})$ ,  $1(\text{Zn}^{\text{II}}, \text{Fe}^{\text{III}})$  is produced, the concentration of which is directly dependent on the amount of  $4(\text{Fe}^{\text{III}})$  that was added to the  $4(\text{Zn}^{\text{II}})$  solution. Photoexcitation of solutions of  $4(\text{Zn}^{\text{II}})$  and  $4(\text{Fe}^{\text{III}})$  provides a decay pathway for  $^1\text{ZnP}^*$  in addition to intrinsic decay because any electron-

ically excited (porphinato)zinc chromophores that are integrated into the supramolecular complex  $1(\text{Zn}^{\text{II}}, \text{Fe}^{\text{III}})$  can be ET quenched by the H bond–associated (porphinato)iron(III) chloride complex; extensive previous studies show that photoinduced ET from  $^1\text{ZnP}^*$  to (porphinato)iron(III) complexes is a primary decay process for  $^1\text{ZnP}^*$  in model compounds that incorporate these donors and acceptors (18, 19).

Scheme 1 shows the kinetic processes rel-



**Scheme 1.**

evant to systems  $1(\text{Zn}^{\text{II}}, \text{Fe}^{\text{III}})$ ,  $2(\text{Zn}^{\text{II}}, \text{Fe}^{\text{III}})$ , and  $3(\text{Zn}^{\text{II}}, \text{Fe}^{\text{III}})$  upon photoexcitation (20). The  $^1k_{\text{ET}}$  rate constants were determined by time-correlated single-photon counting (TCSPC) spectroscopy (21, 22) (Fig. 2). For  $1(\text{Zn}^{\text{II}}, \text{Fe}^{\text{III}})$  (Fig. 2A),  $^1k_{\text{ET}}$  was determined by analysis of the fluorescence decay kinetic profiles of 35  $\mu\text{M}$   $4(\text{Zn}^{\text{II}})$  solutions as a function of  $[4(\text{Fe}^{\text{III}})]$  (brackets denote concentration) (0 to 600  $\mu\text{M}$ ) (23, 24). When  $[4(\text{Fe}^{\text{III}})]$  was nonzero, the observed fluorescence decay was best fit as a biexponential, with kinetic components corresponding to non–H-bond-associated  $4(\text{Zn}^{\text{II}})$  as well as  $1(\text{Zn}^{\text{II}}, \text{Fe}^{\text{III}})$  [Eq. 1, where  $t$  is the time after excitation,  $I$  is the fluorescent intensity,  $k_{\text{int}}$  is the intrinsic decay rate constant of the  $^1\text{ZnP}^*$  in the absence of ET quenching ( $7.04 \times 10^8 \text{ s}^{-1}$ ),  $^1k_{\text{ET}}$  is the photoinduced ET rate constant, and  $\chi_{4(\text{Zn}^{\text{II}})}$  and  $\chi_{1(\text{Zn}^{\text{II}}, \text{Fe}^{\text{III}})}$  are the mole fractions of  $4(\text{Zn}^{\text{II}})$  and  $1(\text{Zn}^{\text{II}}, \text{Fe}^{\text{III}})$  present in solution].

$$I(t)/I(0) = \chi_{4(\text{Zn}^{\text{II}})} \exp[-k_{\text{int}}t] + \chi_{1(\text{Zn}^{\text{II}}, \text{Fe}^{\text{III}})} \exp[-(^1k_{\text{ET}} + k_{\text{int}})t] \quad (1)$$

For every  $4(\text{Fe}^{\text{III}})$  concentration examined, the decay profiles were cleanly biexponential and could be analyzed in terms of the same two exponential lifetimes, 1.42 ns ( $1/k_{\text{int}}$ ) and 114 ps [ $1/(^1k_{\text{ET}} + k_{\text{int}})$ ]. The mole fraction of material undergoing fluorescence decay at 114 ps increased with increasing  $[4(\text{Fe}^{\text{III}})]$ , as expected, because increasing  $[4(\text{Fe}^{\text{III}})]$  results in a decrease in  $[4(\text{Zn}^{\text{II}})]$  with a concomitant increase in  $[1(\text{Zn}^{\text{II}}, \text{Fe}^{\text{III}})]$ . Analysis of these concentration-dependent kinetics data (Fig. 3A) gives an association constant  $K_{\text{assoc}} = 440 \text{ M}^{-1}$  for  $1(\text{Zn}^{\text{II}}, \text{Fe}^{\text{III}})$ . This value is similar in magnitude to that obtained independently by infrared (IR) spectroscopy (Fig. 3B) (15, 25). Consistent with the criteria used in other model systems to evaluate ET rate constants mediated by H-bonded interfaces (11, 12), this experimental system

displays the following properties: (i) No evidence of ET processes other than those in preassociated H-bonded complexes is present, as the 114-ps time constant remained independent of  $[4(\text{Fe}^{\text{III}})]$ ; (ii) when  $4(\text{Fe}^{\text{III}})$  was replaced by [5,10,15,20-tetrakis(3',4',5'-trimethoxyphenyl)porphinato]iron(III) chloride, a complex incapable of H bonding with  $4(\text{Zn}^{\text{II}})$ , only the intrinsic decay process was observed; (iii) because the electronic absorption spectra of mixtures of  $4(\text{Fe}^{\text{III}})$  and  $4(\text{Zn}^{\text{II}})$  appeared as a superposition of the composite monomer spectra without any B-band shifts or broadening, no strong electronic (or excitonic) interaction occurs between the chromophores, as would be expected if  $\pi$ -stacking interactions (aggregation) were significant under these experimental conditions; and (iv) addition of a solvent capable of disrupting H-bonding interactions between  $4(\text{Zn}^{\text{II}})$  and  $4(\text{Fe}^{\text{III}})$ , such as methanol, caused the shorter-lived component in the decay profile to disappear. These facts along with the kinetic data presented enable us to confidently evaluate the  $^1k_{\text{ET}}$  rate constant for the H-bonded supramolecular system  $1(\text{Zn}^{\text{II}}, \text{Fe}^{\text{III}})$  (Table 2).

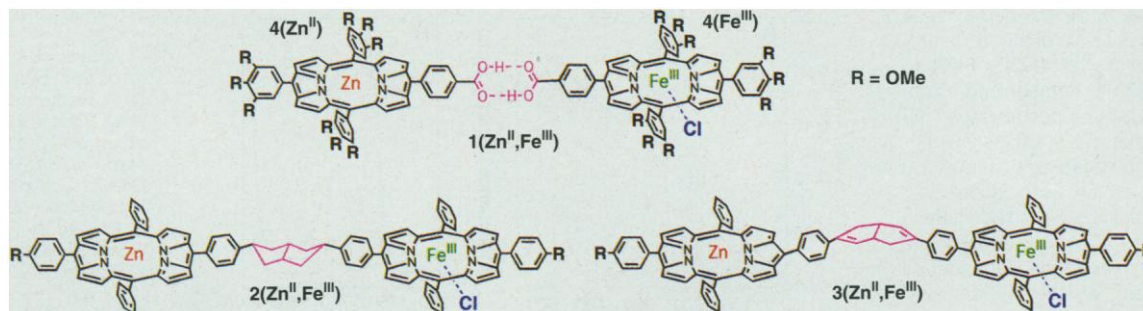
The two covalently linked ET model systems were synthesized from appropriately halogenated (porphinato)zinc precursors through metal-mediated cross-coupling (26–28). Table 2 contrasts the ET rate constants obtained for  $2(\text{Zn}^{\text{II}}, \text{Fe}^{\text{III}})$  and  $3(\text{Zn}^{\text{II}}, \text{Fe}^{\text{III}})$  (Fig. 2B) with that for  $1(\text{Zn}^{\text{II}}, \text{Fe}^{\text{III}})$ . The photoinduced ET rate data for  $1(\text{Zn}^{\text{II}}, \text{Fe}^{\text{III}})$ ,  $2(\text{Zn}^{\text{II}}, \text{Fe}^{\text{III}})$ , and  $3(\text{Zn}^{\text{II}}, \text{Fe}^{\text{III}})$  show that the magnitude of  $^1k_{\text{ET}}$  for  $1(\text{Zn}^{\text{II}}, \text{Fe}^{\text{III}})$ , a supramolecular system featuring weak H-bonding interactions as a key component of the D-to-A ET pathway, exceeds that for  $2(\text{Zn}^{\text{II}}, \text{Fe}^{\text{III}})$  and is comparable to that observed for  $3(\text{Zn}^{\text{II}}, \text{Fe}^{\text{III}})$ , despite having a slightly less exoergic ET reaction than the two covalent ET model systems. Before discussing the role played by the nature of the types of bonds in the bridge in governing the magnitudes of  $^1k_{\text{ET}}$  in supramolecules  $1(\text{Zn}^{\text{II}}, \text{Fe}^{\text{III}})$ ,  $2(\text{Zn}^{\text{II}}, \text{Fe}^{\text{III}})$ , and  $3(\text{Zn}^{\text{II}}, \text{Fe}^{\text{III}})$ , the impact that small deviations in bridge structure and minor differences in reaction driving force have on the photoinduced ET rate constant must be addressed (29, 30).

According to classical and semiclassical ET theory, the ET rate constant  $k_{\text{ET}}$  can be expressed as

$$k_{\text{ET}} = \nu_{\text{N}} \kappa_{\text{E}} \kappa_{\text{N}} \quad (2)$$

where  $\nu_{\text{N}}$  is a nuclear frequency factor,  $\kappa_{\text{E}}$  is an electronic term that describes the D–A electronic coupling (tunneling barrier height), and  $\kappa_{\text{N}}$  is related to the free-energy change  $\Delta G^\circ$  of the reaction (31). The ET driving force in  $1(\text{Zn}^{\text{II}}, \text{Fe}^{\text{III}})$  is 0.17 eV less exoergic than those for

**Fig. 1.** ET model compounds used in this study.



$2(\text{Zn}^{\text{II}}, \text{Fe}^{\text{III}})$  and  $3(\text{Zn}^{\text{II}}, \text{Fe}^{\text{III}})$  (Table 2). Given the relation between  $\kappa_{\text{N}}$  and driving force ( $\Delta G^\circ$ )

$$\kappa_{\text{N}} = \exp[-(\Delta G^\circ + \lambda)^2/4\lambda kT] \quad (3)$$

( $k$  is Boltzmann's constant,  $T$  is temperature, and  $\lambda$  is the total reorganization energy) and the fact that Hoffman has demonstrated that the reorganization energy for ET reactions between excited-state (porphinato)zinc and (porphinato)iron(III) chloride likely exceeds the reaction exoergicities listed in Table 2, primarily because of the changes at the (porphinato)iron(III) site (ligand loss, motion of the Fe with respect to the porphyrin plane, and changes in the porphyrin geometry) that occur concomitant with ET, we expect that  $^1k_{\text{ET}}$  should increase with increasing reaction exoergicities for model complexes  $1(\text{Zn}^{\text{II}}, \text{Fe}^{\text{III}})$ ,  $2(\text{Zn}^{\text{II}}, \text{Fe}^{\text{III}})$ , and  $3(\text{Zn}^{\text{II}}, \text{Fe}^{\text{III}})$  be-

cause  $-\Delta G^\circ < \lambda$  for these systems (32). If driving-force effects dominated the ET kinetics in these systems,  $1(\text{Zn}^{\text{II}}, \text{Fe}^{\text{III}})$  would have the smallest value of  $^1k_{\text{ET}}$ , but this is not the case.

For  $1(\text{Zn}^{\text{II}}, \text{Fe}^{\text{III}})$ ,  $2(\text{Zn}^{\text{II}}, \text{Fe}^{\text{III}})$ , and  $3(\text{Zn}^{\text{II}}, \text{Fe}^{\text{III}})$ , the rigid media that link D to A differ in their orbital hybridization, so the three ET frameworks are nonisostructural (Table 1), which could affect both  $\kappa_{\text{E}}$  and  $\nu_{\text{N}}$ . Such medium structural differences significantly modulate ET rate constants (for a constant number of bonds separating D from A) when D-A orientation or through-space distance is drastically altered (33, 34); in the three ET model systems under consideration here, D-A orientation is not an important variable because it is determined by steric interactions between the bridge phenyl rings and the porphyrin macrocycles, which are identical. Moreover, the differences in the bridge curvature are relatively minor as evinced by the near-constant spatial separation of D and A in  $1(\text{Zn}^{\text{II}}, \text{Fe}^{\text{III}})$ ,  $2(\text{Zn}^{\text{II}}, \text{Fe}^{\text{III}})$ , and  $3(\text{Zn}^{\text{II}}, \text{Fe}^{\text{III}})$ ; thus, any differences in  $^1k_{\text{ET}}$  in these systems must derive from variances in  $\kappa_{\text{E}}$ , and not  $\nu_{\text{N}}$  or  $\kappa_{\text{N}}$ .

The value of  $\kappa_{\text{E}}$  is proportional to the square of the electronic coupling matrix element  $H_{\text{ab}}$ , and  $H_{\text{ab}}$  can be expressed as a function of the electronic coupling matrix element at D-A contact ( $H_{\text{ab}}^\circ$ ) multiplied by the product of a series of decay factors

that correspond to the types of chemical interactions that define the steps in an ET pathway (2). Thus, for an ET pathway composed of both saturated and unsaturated covalent bonds, C<sup>s</sup> and C<sup>u</sup>, as well as hydrogen bonds, H, the electronic coupling matrix element can be represented by

$$H_{\text{ab}} = H_{\text{ab}}^\circ \prod_{i=1}^{N_i} [\text{C}^s] \prod_{j=1}^{N_j} [\text{C}^u] \prod_{k=1}^{N_k} [\text{H}] \quad (4)$$

where [C<sup>s</sup>], [C<sup>u</sup>], and [H] are the decay factors for each of these types of steps in the ET pathway, and the total number of steps in the tunneling pathway is defined as  $N_i + N_j + N_k$ .

Beratan and Onuchic estimate that the tunneling electron wave function decays by a factor of 0.6 as it propagates through a standard covalent bond in a protein. Because the differences in the measured ET rates stem from variations in the respective values of  $\kappa_{\text{E}}$ , we can estimate the decay factor of the tunneling electron wave function across an H-bond interface as 0.51, significantly softer than the  $(0.6)^2$  factor that corresponds to the decay over two standard covalent bonds. This decay factor of 0.51 evaluated for the C=O...H interaction also is a reasonable estimate for the magnitude of the reduction in net D-A coupling when a tunneling electron wave function propagates across a two-bond pathway composed of a C-C single bond and a C=C double bond (35).

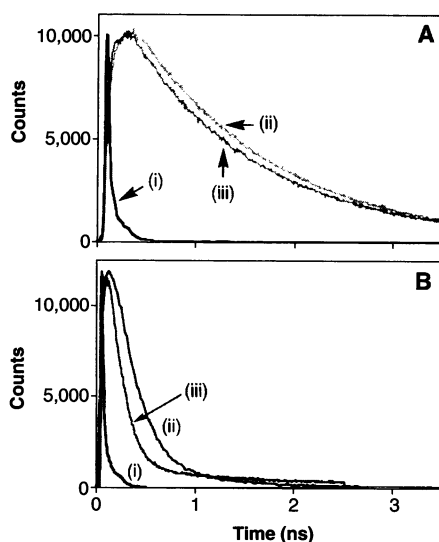


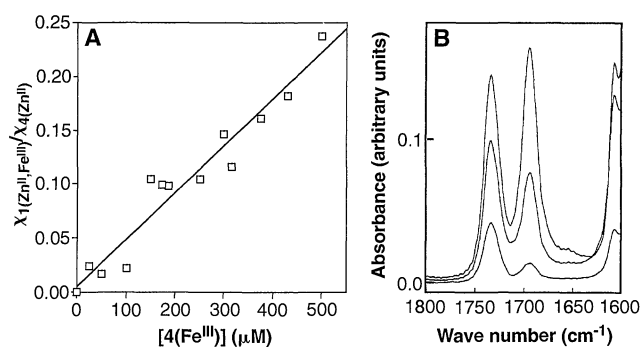
**Fig. 2.** Fluorescence decay profiles obtained by TCSPC. Excitation wavelength  $\lambda_{\text{ex}} = 560$  nm, emission wavelength  $\lambda_{\text{em}} = 640$  nm, solvent =  $\text{CH}_2\text{Cl}_2$ . (A) Sample fluorescence data used to determine the photoinduced ET rate constant in  $1(\text{Zn}^{\text{II}}, \text{Fe}^{\text{III}})$ : (i) instrument response; (ii)  $[\text{4}(\text{Zn}^{\text{II}})] = 35 \mu\text{M}$  and  $[\text{4}(\text{Fe}^{\text{III}})] = 0 \mu\text{M}$ ; (iii)  $[\text{4}(\text{Zn}^{\text{II}})] = 35 \mu\text{M}$  and  $[\text{4}(\text{Fe}^{\text{III}})] = 500 \mu\text{M}$ .  $\chi^2$  (global) = 1.05. (B) Fluorescence data used to determine photoinduced ET rate constant in  $2(\text{Zn}^{\text{II}}, \text{Fe}^{\text{III}})$  and  $3(\text{Zn}^{\text{II}}, \text{Fe}^{\text{III}})$ : (i) instrument response; (ii)  $[\text{2}(\text{Zn}^{\text{II}}, \text{Fe}^{\text{III}})] = 15 \mu\text{M}$  ( $\chi^2 = 1.14$ ); (iii)  $[\text{3}(\text{Zn}^{\text{II}}, \text{Fe}^{\text{III}})] = 15 \mu\text{M}$ ; ( $\chi^2 = 1.28$ ).

**Table 1.** Metrical parameters of the ET model systems. All distances were estimated with MM2 as parameterized within the Personal CaChe program (CaChe Scientific, version 3.5).

ET system	Distance			Orientation
	Through space*	Through bond†	Total pathway bonds‡	Bridge curvature angle (degrees)§
$1(\text{Zn}^{\text{II}}, \text{Fe}^{\text{III}})$	15.0	22.4	14	180
$2(\text{Zn}^{\text{II}}, \text{Fe}^{\text{III}})$	13.9	23.7	14	124
$3(\text{Zn}^{\text{II}}, \text{Fe}^{\text{III}})$	14.4	23.1	14	135

\*Defined as the length of the vector connecting the meso carbons of the (porphinato)zinc and (porphinato)iron(III) chloride moieties bonded directly to the bridge. †Defined as the sum of the lengths of the bonds connecting the meso carbon of the (porphinato)zinc donor bonded directly to the bridge to the central metal atom of the (porphinato)iron(III) chloride acceptor. ‡Defined as the number of bonds that compose the shortest route across the bridge connecting the (porphinato)zinc and the (porphinato)iron(III) chloride moieties at their meso-carbon atoms. §Defined as the angle between the (porphinato)zinc meso carbon, the geometric center of the bridge, and the (porphinato)iron(III) chloride meso carbon. The porphyrin-porphyrin orientation is defined by the porphyrin-meso phenyl torsional angle (14). The geometry of the H-bonded interface was assumed to be identical to that found in benzoic acid dimer x-ray crystal structures, in which  $\angle(\text{O}-\text{H}-\text{O}) \approx 0^\circ$  and the O-O distance  $\approx 2.6 \text{ \AA}$  (37).

**Fig. 3. (A)** The dependence of the ratio of the mole fractions  $\chi$  of **1**(Zn<sup>II</sup>, Fe<sup>III</sup>) to **4**(Zn<sup>II</sup>) (determined from TCSPC spectroscopic kinetic analyses) as a function of **4**(Fe<sup>III</sup>). The slope gives an association constant  $K_{\text{assoc}}$  for **1**(Zn<sup>II</sup>, Fe<sup>III</sup>) = 440 M<sup>-1</sup>. **(B)** Sample concentration dependence data of the IR carbonyl stretching region corresponding to H-bond associated **1**(Zn<sup>II</sup>, Zn<sup>II</sup>) as a function of **4**(Zn<sup>II</sup>) in CH<sub>2</sub>Cl<sub>2</sub>. Analysis of the IR data gives  $K_{\text{assoc}}$  for **1**(Zn<sup>II</sup>, Zn<sup>II</sup>) = 250 M<sup>-1</sup>.



These results have a number of important implications. First, weak chemical interactions can in fact play key roles in mediating biological ET processes. Second, coupling across an H-bond interface is superior to that across two C–C single bonds, the gauge used previously to estimate the maximal coupling through an H bond with an optimal heteroatom-to-heteroatom distance and geometry, which suggests that modification of the theoretical coupling parameters used in such calculations may be in order (2).

Because H bonds involving Asn, Gln, Arg, Asp, and Glu residues as well as the polypeptide backbone feature carbon-to-heteroatom double bonds, the decay of the tunneling electron wave function across the H-bond interfaces defined by these groups within a protein should be estimated as 0.51 and not 0.36, particularly when H-bonding distances and geometries are near their optimal values, in accordance with our experimental results. Use of such a modified coupling parameter for both carbon-to-heteroatom double bonds involved in H-bonding interactions as well as for isolated double bonds in the protein matrix will likely enhance the predictive power of theory to (i) approximate the magnitude of D-A electronic coupling in through-protein ET reactions, (ii) provide insight into the physical path traversed by the tunneling electron in a physiological matrix, and (iii) probe in greater detail how different protein structural regimes manifest disparate electronic coupling.

Given the surprising result that electronic coupling across H-bonded interfaces featuring unsaturated carbon-to-heteroatom junctions is superior to that provided by an interface composed of an analogous number of  $\sigma$  bonds,

**Table 2.** Driving force and ET rate data for the ET model systems (29, 38). Experimental uncertainties in the evaluated rate constants  $^1k_{\text{ET}} < 10\%$ .

ET system	$\Delta G^0$ (eV)	$^1k_{\text{ET}}$ ( $10^9 \text{ s}^{-1}$ )
<b>1</b> (Zn <sup>II</sup> , Fe <sup>III</sup> )	–0.70	8.1
<b>2</b> (Zn <sup>II</sup> , Fe <sup>III</sup> )	–0.87	4.3
<b>3</b> (Zn <sup>II</sup> , Fe <sup>III</sup> )	–0.87	8.8

it is reasonable to envision that electronic coupling mediated through extensive H-bonding networks may be a recurring theme represented in the dominant tunneling pathways of ET proteins. Our results suggest that distinct protein secondary structural motifs will modulate D-A electronic coupling differently. For example, protein coil structure, which satisfies some of its H-bonding requirements with water, would be anticipated to be a rather poor medium to facilitate substantial through-protein electronic coupling because this type of protein secondary structure makes rather inefficient use of the unsaturated heteroatoms capable of forming intraprotein H bonds and thus is less well coupled to the remainder of the protein matrix. Conversely, the data described herein allow one to predict that tunneling over substantial distances across  $\beta$  sheets or through  $\alpha$  helices is more facile than tunneling along the polypeptide backbone. Finally, given the controversies surrounding the interpretation of biological ET rate data (1), the experimental demonstration of differential electronic coupling mediated by H,  $\sigma$ , and  $\pi$  bonds may prove to be a key development in the evolving theoretical framework used to compare and contrast the magnitudes of through-biological matrix ET rate constants in different protein systems (1, 3).

## REFERENCES AND NOTES

- J. R. Winkler and H. B. Gray, *Chem. Rev.* **92**, 369 (1992); C. C. Moser, J. M. Keske, K. Warncke, R. S. Farid, P. L. Dutton, *Nature* **355**, 796 (1992).
- J. N. Onuchic and D. N. Beratan, *J. Chem. Phys.* **92**, 722 (1990); D. N. Beratan and J. N. Onuchic, *Adv. Chem. Ser.* **228**, 71 (1991).
- D. N. Beratan, J. N. Betts, J. N. Onuchic, *Science* **252**, 1285 (1991); J. N. Betts, D. N. Beratan, J. N. Onuchic, *J. Am. Chem. Soc.* **114**, 4043 (1992); D. N. Beratan, J. N. Betts, J. N. Onuchic, *J. Phys. Chem.* **96**, 2852 (1992).
- M. J. Therien, M. Selman, H. B. Gray, I.-J. Chang, J. R. Winkler, *J. Am. Chem. Soc.* **112**, 2420 (1990); M. J. Therien *et al.*, *Adv. Chem. Ser.* **228**, 191 (1991).
- D. S. Wuttke, M. J. Bjerrum, J. R. Winkler, H. B. Gray, *Science* **256**, 1007 (1992); D. R. Casimiro, J. H. Richards, J. R. Winkler, H. B. Gray, *J. Phys. Chem.* **97**, 13073 (1993).
- O. Farver and I. Pecht, *J. Am. Chem. Soc.* **114**, 5764 (1992); L. Qin and N. M. Kostic, *Biochemistry* **32**, 6073 (1993); K. V. Mikkelsen, L. K. Skov, H. Nar, O.

- Farver, *Proc. Natl. Acad. Sci. U.S.A.* **90**, 5443 (1993).
- Ö. Almarsson, A. Sinha, E. Gopinath, T. C. Bruce, *J. Am. Chem. Soc.* **115**, 7093 (1993).
- D. N. Beratan, J. N. Onuchic, J. R. Winkler, H. B. Gray, *Science* **258**, 1740 (1992); H. Pelletier and J. Kraut, *ibid.*, p. 1748; L. Chen, R. C. E. Durlley, F. S. Mathews, V. L. Davidson, *ibid.* **264**, 86 (1994); Z.-w. Chen *et al.*, *ibid.* **266**, 430 (1994); H. B. Brooks and V. L. Davidson, *Biochemistry* **33**, 5696 (1994).
- S. Franzen, R. F. Goldstein, S. G. Boxer, *J. Phys. Chem.* **97**, 3040 (1993).
- K. Bobrowski, J. Holcman, J. Poznanski, M. Ciurak, K. L. Wierzchowski, *ibid.* **96**, 10036 (1992); S. M. Risser, D. N. Beratan, T. J. Meade, *J. Am. Chem. Soc.* **115**, 2508 (1993).
- C. Turró, C. K. Chang, G. E. Leroi, R. I. Cukier, D. G. Nocera, *J. Am. Chem. Soc.* **114**, 4013 (1992).
- A. Harriman, Y. Kubo, J. L. Sessler, *ibid.*, p. 388; J. L. Sessler, B. Wang, A. Harriman, *ibid.* **115**, 10418 (1993).
- In the case of **1**(Zn<sup>II</sup>, Fe<sup>III</sup>), the functionality of the porphyrin phenyl rings was selected to enhance the solubility of the H-bonding components of the supramolecular system. For **1**(Zn<sup>II</sup>, Fe<sup>III</sup>), **2**(Zn<sup>II</sup>, Fe<sup>III</sup>), and **3**(Zn<sup>II</sup>, Fe<sup>III</sup>), reaction driving forces for  $^1k_{\text{ET}}$  have been determined and do not differ significantly (Table 2).
- Molecular modeling studies estimate the meso phenyl-porphyrin torsional angle at 60°, of comparable magnitude to that observed in the solid state [C. K. Schauer, O. P. Anderson, S. S. Eaton, G. R. Eaton, *Inorg. Chem.* **24**, 4082 (1985)]. The barrier to rotation about the meso carbon-to-phenyl bond is substantial, in excess of 15 kcal mol<sup>-1</sup> [S. S. Eaton and G. R. Eaton, *J. Am. Chem. Soc.* **99**, 6594 (1977)].
- Y. I'Haya and T.-i. Shibuya, *Bull. Chem. Soc. Jpn.* **38**, 1144 (1965).
- The [5-(4'-carboxyphenyl)-10,15,20-tris(3'',4'',5''-trimethoxyphenyl)porphyrato]zinc(II), **4**(Zn<sup>II</sup>), and [5-(4'-carboxyphenyl)-10,15,20-tris(3'',4'',5''-trimethoxyphenyl)porphyrato]iron(III) chloride, **4**(Fe<sup>III</sup>), were prepared, isolated, and purified by procedures similar to literature methods (17); so that we could ensure sample integrity, these compounds were subject to flash chromatography on silica immediately before the collection of any kinetic data. Selected characterization data: **4**(Zn<sup>II</sup>): <sup>1</sup>H nuclear magnetic resonance (NMR) spectroscopy (500 MHz, CDCl<sub>3</sub>): chemical shift  $\delta$  12.1 (broad, 1 H), 9.09 (d, 2 H, coupling constant  $J = 4.6$  Hz), 9.07 (m, 4 H), 8.92 (d, 2 H,  $J = 4.6$  Hz), 8.53 (d, 2 H,  $J = 8.0$  Hz), 8.36 (d, 2 H,  $J = 8.0$  Hz), 7.47 (s, 6 H), 4.17 (s, 9 H), 3.95 (s, 18 H). <sup>13</sup>C NMR (60 MHz, CDCl<sub>3</sub>):  $\delta$  172.0, 151.4, 147.8, 137.9, 137.5, 134.6, 131.5, 128.9, 128.6, 120.4, 120.3, 118.6, 112.9, 61.3, 56.4. Visible spectra (vis) (CH<sub>2</sub>Cl<sub>2</sub>): 426 [5.6], 552 [4.27], 589 [3.57]. Fast atom bombardment mass spectrometry (FAB MS): 990 (calculated 990). **4**(Fe<sup>III</sup>): vis (CH<sub>2</sub>Cl<sub>2</sub>): 424 [5.6], 511 [4.2], 578 [3.59], 662 [3.52], 687 [3.52]. FAB MS: 1017 (calculated 1017).
- P. Rothmund and A. R. Menotti, *J. Am. Chem. Soc.* **70**, 1808 (1948); F. R. Longo, M. G. Finarelli, J. B. Kim, *J. Heterocycl. Chem.* **6**, 927 (1968); H. Kobayashi, *Adv. Biophys.* **8**, 191 (1975).
- A. Helms, D. Heiler, G. McLendon, *J. Am. Chem. Soc.* **114**, 6227 (1992).
- R. L. Brookfield, H. Ellul, A. Harriman, *J. Chem. Soc. Faraday Trans. 2* **81**, 1837 (1985); N. Mataga, H. Yao, T. Okada, Y. Kanda, A. Harriman, *Chem. Phys.* **131**, 473 (1989); A. Osuka *et al.*, *J. Am. Chem. Soc.* **112**, 4958 (1990).
- These studies report only  $^1k_{\text{ET}}$  rate data; kinetic analysis of the charge recombination reaction ( $k_{\text{CR}}$ ) is complicated by ligand (Cl<sup>-</sup>) reassociation kinetics (18, 19).
- The TCSPC apparatus has been described in detail elsewhere [G. R. Holtom, *SPIE* **1204**, 1 (1990)]. For these experiments, the excitation wavelength  $\lambda_{\text{ex}}$  = 560 nm, the emission wavelength  $\lambda_{\text{em}}$  = 640 nm, and the full width at half maximum of the instrument response function = 30 ps. Data were analyzed with the Lifetime (Regional Laser and Biotechnology Laboratory, University of Pennsylvania) and Globals Unlimited (Laboratory for Fluorescence Decay, University of Illinois) programs.

22. Time-resolved absorption studies have shown conclusively that the single-exponential decay observed by TCSPC spectroscopy corresponds to the ET quenching rate for similar D-bridge-A systems that feature (porphinato)zinc donors and (porphinato)iron acceptors (18, 19).
23. Samples for transient spectroscopic studies were kept rigorously dry with standard inert-atmosphere techniques. The solids were dried overnight under vacuum at 60°C and then dissolved in dry CH<sub>2</sub>Cl<sub>2</sub> and transferred under nitrogen to a Schlenk-style fluorescence cell to continuously maintain an inert atmosphere throughout the experiment. Sample concentrations were determined by electronic absorption spectroscopy with use of the known extinction coefficients of the compounds.
24. Although the system is a complex mixture of **4(Zn<sup>II</sup>)** and **4(Fe<sup>III</sup>)** monomers as well as **1(Zn<sup>II</sup>, Fe<sup>III</sup>)**, **1(Fe<sup>III</sup>, Fe<sup>III</sup>)**, and **1(Zn<sup>II</sup>, Zn<sup>II</sup>)** dimers in equilibrium, the analysis is simplified by the facts that (i) **4(Fe<sup>III</sup>)** and **1(Fe<sup>III</sup>, Fe<sup>III</sup>)** are nonfluorescent and (ii) maintaining a low concentration of **4(Zn<sup>II</sup>)** (35 μM) guarantees that the concentration of ET-inactive **1(Zn<sup>II</sup>, Zn<sup>II</sup>)** is negligible.
25. The C–O stretching frequencies  $\nu_{CO}$  for **4(Zn<sup>II</sup>)** and **1(Zn<sup>II</sup>, Zn<sup>II</sup>)** are 1735 and 1695 cm<sup>-1</sup>, respectively. The small differences between the  $K_{assoc}$  values obtained from the IR (250 M<sup>-1</sup>) and kinetic studies likely derive from the fact that the IR data were obtained from solutions 2 to 3 orders of magnitude greater in concentration in **4(Zn<sup>II</sup>)** than was used in the TCSPC experiments. Furthermore, for simplicity, **4(Zn<sup>II</sup>)** and **4(Fe<sup>III</sup>)** mixtures were not used in the IR experiments.
26. S. G. DiMugno, V. S.-Y. Lin, M. J. Therien, *J. Am. Chem. Soc.* **115**, 2513 (1993); *J. Org. Chem.* **58**, 5983 (1993); V. S.-Y. Lin, S. G. DiMugno, M. J. Therien, *Science* **264**, 1105 (1994).
27. The synthesis of **2(Zn<sup>II</sup>, Fe<sup>III</sup>)** and **3(Zn<sup>II</sup>, Fe<sup>III</sup>)** are reported in P. J. F. de Rege and M. J. Therien, *Inorg. Chim. Acta*, in press.
28. The mixed-metal supramolecular systems used in our ET studies, **2(Zn<sup>II</sup>, Fe<sup>III</sup>)** and **3(Zn<sup>II</sup>, Fe<sup>III</sup>)**, were synthesized from **2(Zn<sup>II</sup>, Zn<sup>II</sup>)** and **3(Zn<sup>II</sup>, Zn<sup>II</sup>)** by previously reported methods (18, 27). Sample preparation for photophysical studies and analysis of their ET kinetics follow protocols reported in (18).
29. An analogous H-bonding D-A complex **5(Zn<sup>II</sup>, Fe<sup>III</sup>)** was assembled with [5-(4'-carboxyphenyl)-10,15,20-tris(4''-methoxyphenyl)porphinato]zinc(II), **6(Zn<sup>II</sup>)**, and [5-(4'-carboxyphenyl)-10,15,20-tris(4''-methoxyphenyl)porphinato]iron(III) chloride, **6(Fe<sup>III</sup>)**, as components. The driving force and evaluated ET rate constants were -0.99 eV and  $6.2 \times 10^{-9} \text{ s}^{-1}$ . Because this ET reaction is more exoergic than those of **2(Zn<sup>II</sup>, Fe<sup>III</sup>)** and **3(Zn<sup>II</sup>, Fe<sup>III</sup>)** and because the slightly smaller ET rate constant for **5(Zn<sup>II</sup>, Fe<sup>III</sup>)** relative to **1(Zn<sup>II</sup>, Fe<sup>III</sup>)** may derive from the onset of Marcus inverted region effects, we chose **1(Zn<sup>II</sup>, Fe<sup>III</sup>)** as the benchmark for comparison with **2(Zn<sup>II</sup>, Fe<sup>III</sup>)** and **3(Zn<sup>II</sup>, Fe<sup>III</sup>)**. The less exoergic **1(Zn<sup>II</sup>, Fe<sup>III</sup>)** thus sets a lower limit for relative coupling enhancement provided by a H-bond interface relative to one composed entirely of  $\sigma$  bonds. The evaluated rate constants for the photoinduced ET reactions of both the less exoergic **1(Zn<sup>II</sup>, Fe<sup>III</sup>)** and the more exoergic **5(Zn<sup>II</sup>, Fe<sup>III</sup>)** exceed that evaluated for **2(Zn<sup>II</sup>, Fe<sup>III</sup>)**.
30. Significantly different librational motions of the bridge with respect to D and A can also attenuate electronic coupling. Two such types of motion need to be considered. The first involves librations about the porphyrin-to-phenyl bond that is part of the ET pathway. It is known that the magnitude of electronic coupling follows an approximate  $\cos \theta$  dependence, where  $\theta$  is the dihedral angle between the porphyrin and aryl planes; the fact that single exponential decay is observed in the ET kinetics for such systems reflects a rate constant for the "average" electronic coupling provided by the distribution of angles  $\theta$  accessible in solution [L. R. Khundkar, J. W. Perry, J. E. Hanson, P. B. Dervan, *J. Am. Chem. Soc.* **116**, 9700 (1994); D. N. Beratan, *ibid.* **108**, 4321 (1986); (18)]. Because the distribution of dihedral angles  $\theta$  will be the same for compounds **1(Zn<sup>II</sup>, Fe<sup>III</sup>)**, **2(Zn<sup>II</sup>, Fe<sup>III</sup>)**, and **3(Zn<sup>II</sup>, Fe<sup>III</sup>)**, the electronic coupling between the porphyrin and the meso aryl group is invariant. Similarly, the calculated barriers to rotation of the central portion of each bridge with respect to its pendant aryl rings is  $\sim 3.0 \text{ kcal mol}^{-1}$  (MOPAC 6.0; J. J. P. Stewart, Frank J. Seiler Research Laboratory, U.S. Air Force Academy). Rotation about the central portion of the bridge is thus similarly fast in all three systems; to first approximation, bridge dynamics cannot account for the observed differences in coupling.
31. R. A. Marcus and N. Sutin, *Biochim. Biophys. Acta* **811**, 265 (1986).
32. S. E. Peterson-Kennedy, J. L. McGourty, J. A. Kalweit, B. M. Hoffman, *J. Am. Chem. Soc.* **108**, 1739 (1986).
33. G. L. Closs and J. R. Miller *Science* **240**, 440 (1988); M. R. Wasielewski, *Chem. Rev.* **92**, 435 (1992).
34. Y. Sakata *et al.*, *Chem. Lett.* **1991**, 1307 (1991); Y. Sakata *et al.*, *J. Am. Chem. Soc.* **111**, 8979 (1989).
35. Recent work by Miller also indicates that the introduction of a C=C double bond into an otherwise saturated bridge leads to enhanced D-A coupling relative to that found for the purely aliphatic ET medium, even when the point of unsaturation is well separated from both D and A (B. P. Paulson, W.-X. Gan, G. L. Closs, J. R. Miller, in preparation).
36. M. R. Wasielewski, M. P. Niemczyk, W. A. Svec, E. B. Pettitt, *J. Am. Chem. Soc.* **107**, 1080 (1985); A. D. Joran *et al.*, *Nature* **327**, 508 (1987); G. L. Gaines III, M. P. O'Neil, W. A. Svec, M. P. Niemczyk, M. R. Wasielewski, *J. Am. Chem. Soc.* **113**, 719 (1991).
37. M. Colapietro and A. Domenicano, *Acta. Crystallogr. B* **38**, 1953 (1982); *ibid.* **34**, 3277 (1978).
38. Driving force ( $\Delta G^\circ$ ) was calculated from appropriate electrochemical parameters and the  $E_{O-O}$  values (<sup>1</sup>ZnP<sup>+/</sup>ZnP) for the (porphinato)zinc chromophores, which are defined as the mean of the Q(0, 0) energy and the highest energy emission wavelength (36). For **1(Zn<sup>II</sup>, Fe<sup>III</sup>)**, electrochemical and photophysical parameters were based on measurements carried out with **4(Fe<sup>III</sup>)** and **4(Zn<sup>II</sup>)**: (ZnP<sup>+/</sup>ZnP) = 830 mV; (Fe<sup>III</sup>P/Fe<sup>II</sup>P) = -560 mV; (<sup>1</sup>ZnP<sup>+/</sup>ZnP) = 2.09 eV. For **2(Zn<sup>II</sup>, Fe<sup>III</sup>)** and **3(Zn<sup>II</sup>, Fe<sup>III</sup>)**, electrochemical and photophysical parameters were based on measurements carried out with [5-(4'-methoxyphenyl)-15-(4''-iso-propylphenyl)-10,20-diphenylporphinato]zinc(II) and [5-(4'-methoxyphenyl)-15-(4''-iso-propylphenyl)-10,20-diphenylporphinato]iron(III) chloride, which served as model compounds for the covalent supramolecular ET systems: (ZnP<sup>+/</sup>ZnP) = 740 mV; (Fe<sup>III</sup>P/Fe<sup>II</sup>P) = -490 mV; (<sup>1</sup>ZnP<sup>+/</sup>ZnP) = 2.10 eV. Cyclic voltammetric experimental conditions: [porphyrin] = 1 mM; [TBAPF<sub>6</sub>] or [TBAC] = 0.10 M (TBA, tetra-*n*-butylammonium); solvent = CH<sub>2</sub>Cl<sub>2</sub>; scan rate = 0.5 V s<sup>-1</sup>; standard calomel reference electrode, 0.1-μm platinum disk working electrode; internal standard = ferrocene/ferrocenium (Fe<sup>II</sup>/Fe<sup>III</sup>) redox couple = 430 mV. TBAPF<sub>6</sub> was the supporting electrolyte used in the determination of the ZnP<sup>+/</sup>ZnP redox couples, whereas TBACI was used as the supporting electrolyte when Fe<sup>III</sup>P/Fe<sup>II</sup>P electrochemical potentials were evaluated.
39. Kinetic measurements were performed at the NIH-supported Regional Laser and Biotechnology Laboratory (RLBL) at the University of Pennsylvania. The authors thank L. G. Jahn for his assistance with these measurements. P. J. F. D. thanks the National Science and Engineering Research Council of Canada for a postgraduate fellowship. This work was supported by the Searle Scholars Program (Chicago Community Trust) and the U.S. Department of Energy (DE-FG02-94ER14494). M. J. T. is extremely grateful to the Arnold and Mabel Beckman Foundation, E. I. du Pont de Nemours, and the National Science Foundation for Young Investigator Awards, as well as the Alfred P. Sloan Foundation for a research fellowship.

17 March 1995; accepted 13 July 1995

## Synchrony and Causal Relations Between Permian-Triassic Boundary Crises and Siberian Flood Volcanism

Paul R. Renne,\* Zhang Zichao, Mark A. Richards, Michael T. Black,† Asish R. Basu

The Permian-Triassic boundary records the most severe mass extinctions in Earth's history. Siberian flood volcanism, the most profuse known such subaerial event, produced 2 million to 3 million cubic kilometers of volcanic ejecta in approximately 1 million years or less. Analysis of <sup>40</sup>Ar/<sup>39</sup>Ar data from two tuffs in southern China yielded a date of 250.0 ± 0.2 million years ago for the Permian-Triassic boundary, which is comparable to the inception of main stage Siberian flood volcanism at 250.0 ± 0.3 million years ago. Volcanogenic sulfate aerosols and the dynamic effects of the Siberian plume likely contributed to environmental extrema that led to the mass extinctions.

Continental flood volcanism produced episodic outpourings of magma, chiefly basalt, whose volumes (up to 3.0 × 10<sup>6</sup> km<sup>3</sup>) and

mean eruption rates [up to 3 km<sup>3</sup>/year sustained for ~1 million years (My)] are significantly larger than those of volcanism in other geologic settings (1). Causal relations between flood volcanism and mass extinctions have been postulated for more than a decade (2, 3), in part because of the apparent coincidence between the two most profound mass extinctions known (Permian-Triassic and Cretaceous-Tertiary) and two of the most extensive continental flood volcanism events (Siberian and Deccan traps, respectively). Likely mechanisms of mass mortality (3–5) posed by flood basalts include global cooling caused by sulfate aero-

P. R. Renne and M. T. Black, Berkeley Geochronology Center, 2455 Ridge Road, Berkeley, CA 94709, USA. Z. Zichao, Yichang Institute of Geology and Mineral Resources, Post Office Box 502, Yichang 443003, People's Republic of China. M. A. Richards, Department of Geology and Geophysics, University of California, Berkeley, CA 94720, USA. A. R. Basu, Department of Earth and Environmental Sciences, University of Rochester, Rochester, NY 14627, USA.

\*To whom correspondence should be addressed.

†Present address: Department of Biological Anthropology and Anatomy, Duke University, Durham, NC 27706, USA.